nature communications

Article

https://doi.org/10.1038/s41467-025-63454-7

Induction of experimental cell division to generate cells with reduced chromosome ploidy

Received: 27 February 2025

Accepted: 25 July 2025

Published online: 30 September 2025

Check for updates

Nuria Marti Gutierrez[1], Aleksei Mikhalchenko[1], Maria Shishimorova[1], Daniel Frana[1], Crystal Van Dyken[1], Ying Li[1], Hong Ma[1], Amy Koski[1], Dan Liang[1,4], Sang-Goo Lee[1], Daniel Eyberg[1], Zahra Safaei[1], Eunju Kang[2], Yeonmi Lee[2], Thomas O'Leary[3], David Lee[3], Sacha Krieg[3], Diana Wu[3], Elizabeth Rubin[3], Paula Amato[1,3] ✉ & Shoukhrat Mitalipov[1] ✉

Somatic cell nuclear transfer (SCNT) enables the direct reprogramming of somatic cells into functional oocytes, albeit with a diploid genome. To address ploidy reduction, we investigated an experimental reductive cell division process, termed *mitomeiosis*, wherein non-replicated (2n2c) somatic genomes are prematurely forced to divide following transplantation into the metaphase cytoplasm of enucleated human oocytes. However, despite fertilization with sperm, SCNT oocytes remained arrested at the metaphase stage, indicating activation failure. Artificial activation using a selective cyclin-dependent kinase inhibitor successfully bypassed this arrest, inducing the segregation of somatic chromosomes into a zygotic pronucleus and a polar body. Comprehensive chromosome tracing via sequencing revealed that homologous chromosome segregation occurred randomly and without crossover recombination. Nonetheless, an average of 23 somatic chromosomes were retained within the zygote, demonstrating the feasibility of experimentally halving the diploid chromosome set. Fertilized human SCNT oocytes progressed through normal embryonic cell divisions, ultimately developing into embryos with integrated somatic and sperm-derived chromosomes. While our study demonstrates the potential of mitomeiosis for in vitro gametogenesis, at this stage it remains just a proof of concept and further research is required to ensure efficacy and safety before future clinical applications.

Infertility affects millions of individuals worldwide and is often caused by the absence of functional gametes. In women, age-related decline in oocyte quality and quantity has been recognized as a primary contributing factor to infertility, particularly after their mid-thirties[1]. In vitro fertilization (IVF) is ineffective for patients lacking functional gametes, leaving them with no option to have genetically related children except through the use of donor gametes.

Reprogramming a patient's somatic cells into induced pluripotent stem cells (iPSCs), followed by differentiation into functional sperm or oocytes—a concept known as in vitro gametogenesis (IVG)—holds

[1]Center for Embryonic Cell and Gene Therapy, Oregon Health & Science University, Portland, OR 97239, USA. [2]Department of Biomedical Science and CHA Advanced Research Institute, CHA University, Gyeonggi-do, Republic of Korea. [3]Division of Reproductive Endocrinology and Infertility, Department of Obstetrics and Gynecology, Oregon Health & Science University, Portland, OR 97239, USA. [4]Present address: Department of Obstetrics and Gynecology, the First Affiliated Hospital of Anhui Medical University, Hefei, Anhui, China. ✉e-mail: amatop@ohsu.edu; shoukhrat@gmail.com

immense therapeutic potential, especially for patients without viable gametes. Proof-of-concept for female IVG has been established in mouse models[2]; however, due to significant differences in germ cell development between mice and humans, the translation of IVG to human oocytes remains elusive. Unlike the differentiation of iPSCs into adult somatic cells, IVG-derived oocytes must acquire maternal cytoplasmic factors essential for inducing totipotency after fertilization. They must also undergo proper meiotic recombination, chromosome ploidy reduction, and imprint reprogramming to meet the requirements for future clinical applications. Notably, the natural development of human oocytes from pluripotent progenitors within an embryo is a lengthy process, taking more than a decade to reach functional maturity. For clinical applications, IVG must substantially shorten this timeline to a few weeks.

Functional oocytes can also be generated through direct reprogramming of somatic cells via donor oocyte cytoplasm following somatic cell nuclear transfer (SCNT)[3,4]. SCNT-based IVG could offer several advantages, including reprogramming of transplanted somatic cell genomes directly to the oocyte-like epigenome by natural oocyte cytoplasmic factors[5,6]. Furthermore, the cytoplasm of in vivo matured donor oocytes provides essential maternal factors and germline mitochondria critical for subsequent induction of totipotency and full-term development of SCNT embryos.

Since the cytoplasm of enucleated metaphase II (MII)-arrested oocytes retains metaphase activity, implanted somatic chromatin rapidly condenses to form a metaphase-like spindle, resulting in the establishment of an MII-arrested SCNT oocyte[7,8]. Given that SCNT oocytes are diploid, fertilization with sperm has not been considered due to the risk of triploidy. Conventional SCNT applications instead utilize artificial activation to induce exit from metaphase arrest while preventing cytokinesis and chromosome loss[9,10]. Simultaneously, artificial activation triggers the release of maternal cytoplasmic factors responsible for inducing totipotency and initiating embryonic mitotic cycles. The developmental potential of SCNT oocytes has been well demonstrated by the successful production of live cloned mammals and the generation of functional human blastocysts and embryonic stem cells (SCNT-ESCs)[8].

With the ultimate goal of developing infertility treatments for individuals without functional oocytes, we recently demonstrated that ploidy reduction can be experimentally achieved in mouse SCNT oocytes following fertilization with sperm[11]. Our findings indicated that premature metaphase spindles, comprising single-chromatid chromosomes formed after transplanting non-replicated, G0/G1-arrested somatic cell nuclei into enucleated MII oocytes, are capable of discarding one set of parental homologs into a pseudo polar body (PB) upon fertilization[12]. SCNT zygotes consisting of haploid somatic and sperm pronuclei can develop into diploid embryos and produce live mouse offspring[11,12].

In this study, we adapted mitomeiosis for human SCNT oocytes and investigated whether metaphase spindles are functional and capable of discarding somatic chromosomes into the PB upon fertilization or artificial activation. We conducted precise chromosome sequencing to trace homologous chromosome segregation and examine ploidy reduction mechanisms. Lastly, we evaluated the integration of somatic and sperm chromosomes in preimplantation embryos derived from fertilized human SCNT oocytes.

Results

Human SCNT oocytes containing nonreplicated somatic chromosomes remain arrested at metaphase II upon fertilization

Typical mitotic and meiotic cell divisions are preceded by a single round of DNA replication during the S-phase of the cell cycle resulting in duplication of chromosomes to two sister chromatids (2n4c; Fig. 1a, b). In the mitotic metaphase, sister chromatids from each chromosome are pulled to opposite poles of the spindle and segregated upon cytokinesis into two genetically identical daughter cells with a diploid number of chromosomes (2n2c). In contrast, during the female meiotic metaphase I, homologous chromosomes are paired with each other within a spindle and separated upon reductional division to haploid daughter cells, i.e. an oocyte and a polar body 1 (PB1), each containing one copy of each homolog (1n2c). Since chromosomes still contain two sister chromatids, the second meiotic division bypasses the S-phase and directly enters metaphase II (MII) and remains arrested at MII until fertilization with sperm. Upon fertilization, an MII oocyte exits from metaphase arrest and similar to mitosis, segregates sister chromatids to the female pronucleus (PN) and the PB2 (1n1c; Fig. 1a).

We recently modified the conventional mouse SCNT and induced an experimental reductive cell division by mitomeiosis (Fig. 1b)[11,12]. Progression through various cell cycle stages is strictly regulated by DNA integrity checkpoint regulatory mechanisms including S/G2 and G2/M checkpoints. These checkpoints play a crucial role in ensuring that the metaphase does not commence if DNA replication is incomplete[13,14]. In meiosis, the cell cycle checkpoint blocks progression from metaphase to anaphase if positions of chromosomes and formation of a proper bipolar spindle are compromised[15]. Therefore, we initially investigated if nonduplicated G0/G1 (2n2c) genomes of human fibroblasts can prematurely enter the metaphase upon nuclear transfer into enucleated, MII-arrested cytoplasm of human oocytes. In vivo matured oocytes were collected following routine clinical ovarian stimulation and retrieval from young, healthy egg donor volunteers after obtaining informed consent[8].

Spindle-chromosomal complexes from 270 mature, MII-arrested oocytes containing the PB1 were removed shortly after retrieval and cytoplasts were fused with G0/G1-arrested fibroblasts following our previously developed methods[8]. Premature onset of metaphase was monitored by observation of de novo spindle formation in SCNT oocytes using noninvasive imaging under polarized microscope equipped with the Oosight system[8]. Visible spindles, similar to those seen in control intact MII oocytes, became first detectable in SCNT oocytes 1 h after fusion, but the majority of spindles (77.5% ± 4.8) appeared after 2 h (Fig. 2a). Spindle images were captured, and their size and morphology analyzed by Oosight Meta software. SCNT spindles were elongated in shape and measurements of length and width were similar to spindles in intact MII oocytes (Fig. 2b, c).

Selected SCNT oocytes were fixed at several critical time points and immunolabeled to visualize spindle microtubules (α-tubulin), chromosome centromeres (kinetochore), and stained with DAPI (for DNA). These oocytes were then imaged under fluorescence microscopy to monitor spindle formation dynamics. Somatic cell nuclei in the interphase stage persisted in SCNT oocytes for up to 30 min post-fusion (Fig. 2d). By 1 h, SCNT oocyte nuclei underwent nuclear envelope breakdown (NEBD), premature chromatin condensation (PCC), and initiated microtubule formation (Fig. 2d). Bipolar SCNT spindles, with chromosome centromeres positioned at the equatorial region similar to control MII oocytes, were observed 2 h post-fusion (Fig. 2d, Supplementary Movie 1, 2). However, abnormal spindle morphology was also noted in majority of SCNT oocytes including small, round, or multipolar configurations (Fig. 2e).

These findings provide important insights into spindle formation dynamics during mitomeiosis in human oocytes and support our conclusion that, following fusion with enucleated MII oocyte cytoplasm, somatic 2n2c chromatin directly enters metaphase, bypassing the natural S-phase.

Next, we asked if human SCNT oocytes can exit from the MII-arrest and segregate non-duplicated chromosomes consisting of single chromatids to daughter cells. Naturally, mature MII oocytes remain arrested at the metaphase until fertilization with sperm which triggers exit from metaphase and sister chromatid segregation into the PB2 and the female PN, a signaling mechanism commonly referred to as oocyte activation. Intact control MII ($n = 30$) and SCNT oocytes ($n = 41$)

https://doi.org/10.1038/s41467-025-63454-7

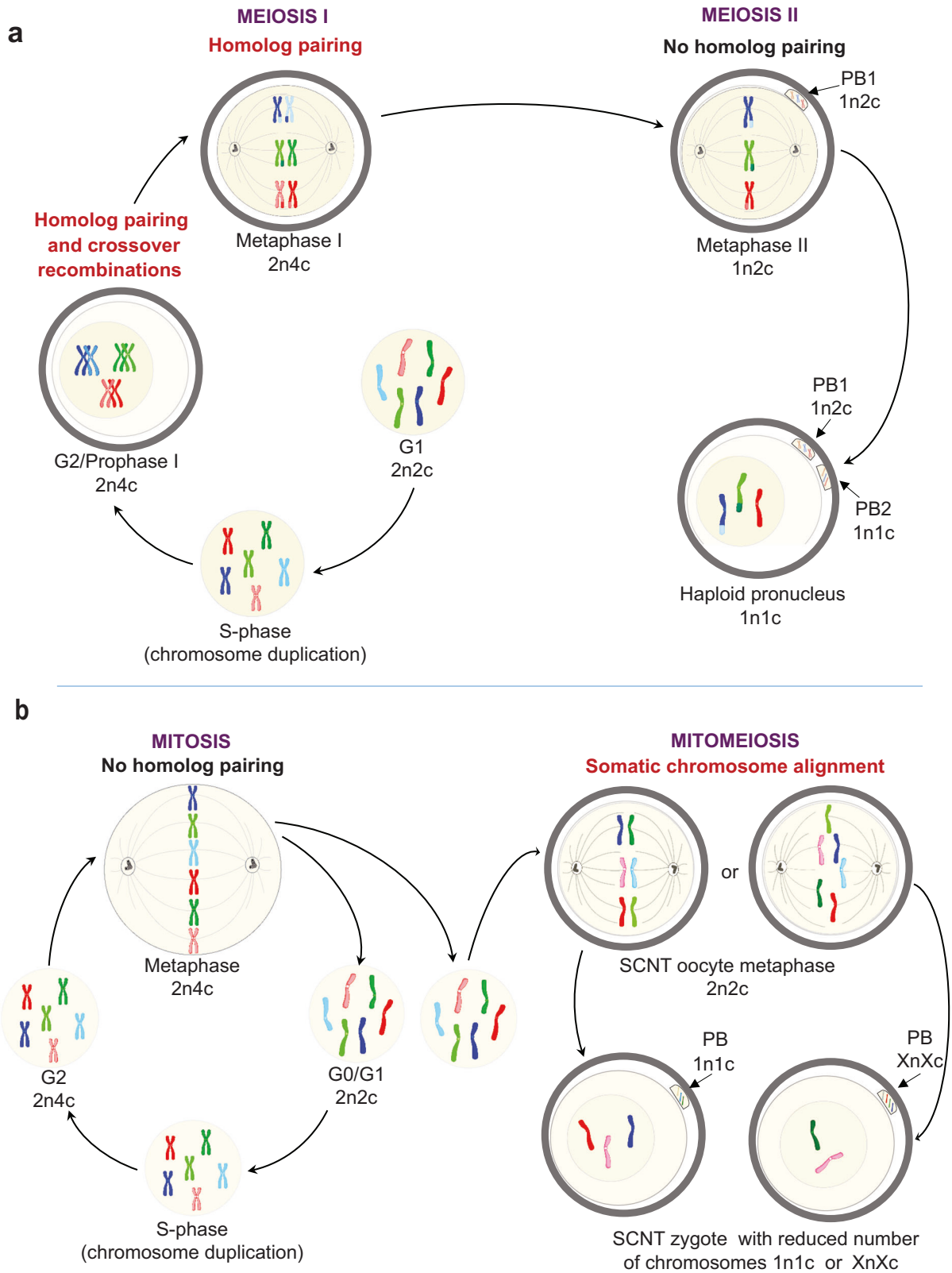

with visible spindles were fertilized with sperm donated by a healthy research donor using intracytoplasmic sperm injection (ICSI). In the control group, 82.9% ± 9.5 fertilized oocytes extruded the PB2 and 79.8% ± 9.2 formed two PNs (female and male) visible after 6 h post fertilization (Fig. 2f). In contrast, only 23.4% ± 8.7 of sperm injected SCNT oocytes extruded the PB and 17.4% ± 9.3 formed PNs but PN formation was delayed up to 12 h post ICSI. While all control zygotes cleaved and 59% ± 16.1 reached blastocysts, only 25% of SCNT zygotes cultured cleaved but arrested at the 2-cell stage (Fig. 2f). It is important to note that the 25% activation rate refers specifically to PB extrusion, representing completion of the second division in mitomeiosis, rather than failure of subsequent mitotic cleavage.

These results indicate that a nonduplicated (2n2c) genome can enter prematurely into metaphase when nuclei of G0/G1 somatic cells

Fig. 1 | Ploidy reduction by mitomeiosis. A schematic cell cycle and chromosome segregation mechanisms to daughter cells during canonical mitosis, meiosis I and meiosis II vs. mitomeiosis, an experimental reductive cell division induced in non-duplicated (2n2c) somatic cell genomes. Created in BioRender. Marti, N. (2025). **a** Chromosome dynamics and segregation during two consecutive meiotic cell divisions. Left panel shows the reductive meiosis I, where the duplicated homologous chromosomes consisting of sister chromatids pair, synapse and crossover followed by their segregation to the MII oocyte and its PB1. Right panel depicts the second meiotic division, where, similar to mitosis, sister chromatids segregate to the zygote and its PB2. **b** Left panel presents the canonical mitotic cell cycle, where following chromosome duplication, sister chromatids of each chromosome are segregated into two daughter cells maintaining the diploid chromosome content during cell divisions. Right panel demonstrates reductive mitomeiosis, where the nucleus at the G0/G1 stage is transferred into the cytoplasm of enucleated MII oocyte, thus bypassing the S-phase and prematurely entering the metaphase. The residual metaphase activity of enucleated MII-arrested oocyte forces premature condensation of non-duplicated chromosomes and formation of bipolar mitomeiosis spindle. Depending on chromosome positioning and attachment to the spindle, subsequent segregation of chromosomes to the zygote and the PB can result in either randomly reduced ploidy or haploidy in daughter cells.

are directly transplanted into enucleated MII-arrested oocyte cytoplasm. However, natural, sperm-induced activation is insufficient to release SCNT oocytes from the MII arrest. As the percentage of abnormal spindles did not directly correlate with the 77% that failed polar body extrusion upon sperm fertilization, it may be reasonable to suggest that additional factors beyond spindle morphology contribute to activation failure.

Release from metaphase arrest and chromosome segregation in human SCNT oocytes induced by assisted activation

While the exact mechanisms responsible for failed fertilization of SCNT oocytes remain unclear, we reasoned that the persistent metaphase arrest could be due to failed activation. MII arrest is maintained by high activity of Maturation Promoting Factor (MPF) consisting of cyclin-dependent protein kinase 1 (Cdk1) and cyclin B (Fig. 3a)[16,17]. Sperm entry during fertilization triggers Ca^{2+} oscillations leading to degradation of cyclin B and subsequently inactivation of Cdk1 and exit from the MII arrest[18]. Alternatively, exit from the MII arrest can be induced experimentally, following so called artificial oocyte activation approaches[10]. Artificial activation is a critical step for conventional SCNT allowing exit from the MII arrest in SCNT oocytes without fertilization with sperm and thus avoiding possible triploidy. In addition to exit from the MII arrest, conventional activation procedures also block cytokinesis in SCNT oocytes preventing chromosome segregation into PBs[10]. We previously established sequential artificial activation stimuli critical for human SCNT oocytes to exit from the MII arrest and develop to blastocysts and SCNT-ESCs[8]. However, implementation of 6-dimethylaminopurine (6-DMAP), a broad protein phosphorylation inhibitor for conventional SCNT activation also prevents cytokinesis and PB extrusion[10].

Therefore, we tested an alternative activation for the ability to induce exit from the metaphase arrest without interfering with cytokinesis and PB extrusion. We initially mimicked calcium elevations by electroporation of MII and SCNT oocytes in Ca^{2+}-containing D-sorbitol buffer[8] and monitored release from the MII arrest. Electroporation alone induced robust cytokinesis and PB2 extrusion in the control MII oocyte group, but pronuclear formation was significantly delayed (10–12 h) compared to that seen in sperm fertilized zygotes (6 h). Moreover, all zygotes failed to cleave and remained arrested at the 1-cell stage (Fig. 3b). Upon electroporation, only 16.7% ± 10.5 of SCNT oocytes extruded the PB and 13.3% ± 9.7 formed one PN also visible late, 10–12 h after electroporation. Similar to controls, all SCNT zygotes failed to cleave (Fig. 3b).

Generally, calcium elevations alone are not sufficient to induce release from the MII arrest and initiate embryonic mitotic cycles[10]. Additional stimuli are required to inactivate MPF in human or monkey MII oocytes. Therefore, we treated control intact MII ($n = 15$) and SCNT ($n = 74$) oocytes with electroporation followed by 4-h incubation with roscovitine, a selective cyclin-dependent kinase inhibitor, in order to downregulate MPF activity while also allowing cytokinesis and PB extrusion (Fig. 3a)[10,19]. In the control MII group, 83.3% ± 10.5 oocytes extruded the PB2 and formed a single PN, 6–7 h after electroporation (Fig. 3b). In SCNT group treated with this sequential activation, 68.6% ± 7 of oocytes extruded the PB and 57.7% ± 6.2 formed a single PN, visible within 6–7 h after electroporation (Fig. 3b, c; Supplementary Movie 3). Imaging of immunolabelled SCNT oocytes 1 h after activation demonstrated an anaphase-like microtubule arrangement with somatic chromosomes situated at both poles of the spindle (Fig. 2d).

The majority of zygotes in both control and SCNT groups cleaved (91.7% ± 4.6 and 93.8% ± 6.3, respectively) and while 45.8% ± 16.2 of control (parthenogenetic) embryos reached the blastocyst stage, SCNT embryos arrested at the 4-10-cell stage.

To determine if this artificial activation can rescue SCNT oocytes from the MII arrest upon fertilization with sperm. Control MII ($n = 30$) and SCNT ($n = 82$) oocytes were fertilized with sperm by ICSI and then SCNT oocytes activated with electroporation+roscovitine. The majority of control and SCNT oocytes extruded polar bodies (82.9% ± 9.5 and 77.9% ± 4.9, respectively) and formed two pronuclei (79.8% ± 9.2 and 76% ± 5.5, respectively) after 6–7 h post fertilization (Fig. 3d, e). All control and most SCNT zygotes with 2 PNs cleaved (100% and 83.3% ± 16.7, respectively), while 59% ± 16.1 of control embryos reached the blastocyst stage, only 8.8% ± 5.2 fertilized SCNT embryos developed to blastocysts (Fig. 3d, e).

Our results showed that supplemental activation with electroporation and roscovitine can rescue the fertilization by sperm and release SCNT oocytes from the MII arrest. Moreover, this artificial activation does not affect normal fertilization nor development of control, intact MII oocytes suggesting its potential applications for assisted activation for IVF cases with fertilization failures. In summary, a diploid but non-replicated somatic genome (2n2c) can be forced to enter prematurely into a metaphase of mitomeiosis by SCNT. Moreover, upon assisted activation, SCNT oocytes consisting of 2n2c somatic chromosomes can bypass spindle checkpoint arrest and resume embryonic cell divisions.

Chromosome segregation patterns and ploidy reduction in SCNT zygotes following mitomeiosis

Next, we asked how 2n2c somatic chromosomes in human SCNT oocytes are segregated to daughter cells (i.e. PN and PB) upon exit from metaphase of mitomeiosis. To identify all human chromosomes and distinguish somatic parental homologs from each other and from sperm (total of 69 chromosomes), we developed a custom, whole chromosome tracing approach using an amplicon sequencing assay (Ampliseq). A family consisting of parents from diverse ethnic backgrounds and their daughter were recruited to participate in this research, as was an unrelated research sperm donor who also provided blood DNA and skin biopsies for this study. Initially, WGS was performed on genomic DNA from all four study subjects and screened for presence of unique SNVs discriminating maternal and paternal somatic chromosomes from sperm homologs. WGS data were then analyzed to identify informative triallelic loci on all autosomal and X chromosomes that would allow distinction between maternal and paternal chromosomes in SCNT oocytes generated from daughter's skin fibroblasts from sperm homologs in fertilized SCNT embryos. We selected a total of 630 highly confident loci covering 584 triallelic and 47 biallelic genomic variants in autosomal and X chromosomes and used this database to build the targeted AmpliSeq sequencing platform. We

https://doi.org/10.1038/s41467-025-63454-7

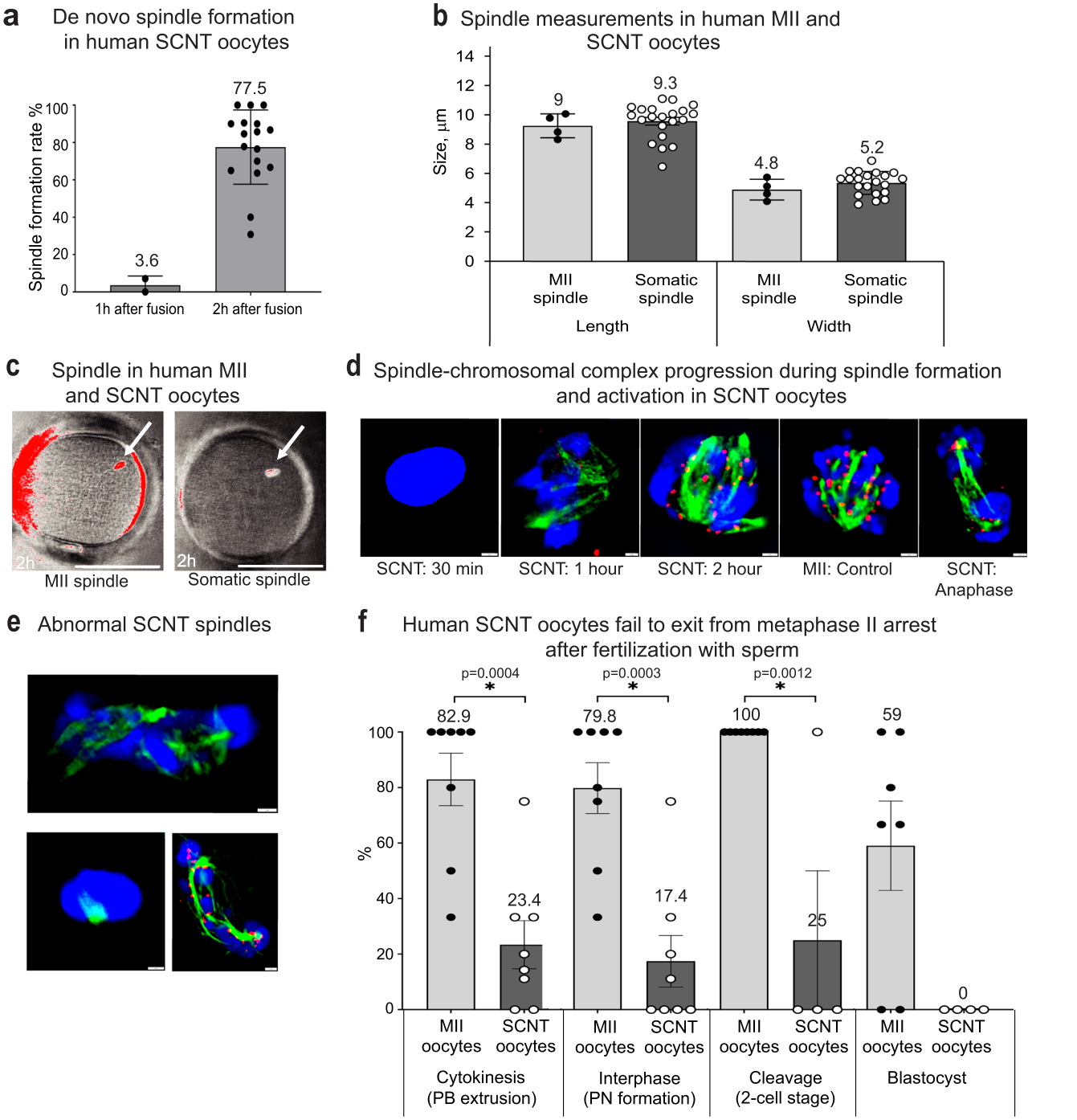

Fig. 2 | Somatic nuclei containing nonreplicated (2n2c) genomes can enter prematurely the metaphase upon transfer to MII cytoplasts but do not respond to sperm induced activation. a De novo spindles formed in SCNT oocytes become clearly visible after 2 h post fusion. Black dots in the graph indicate individual values. 1 h group: 28 SCNT oocytes examined over 2 independent experiments. 2 h group: 215 SCNT oocytes were examined over 17 independent experiments. Error bars represented as SEM. **b** Spindle size measurements in control MII and SCNT oocytes using Oosight imaging. Bar plots show average length and width of spindles measured in control MII ($n = 4$) and SCNT ($n = 21$) oocytes. Black and white dots in the graph indicate individual values. Error bars represented as SEM. **c** Spindle morphology visualized with Oosight live imaging. Upper-left, control MII oocyte with typical spindle image. Upper-right, SCNT oocyte spindle with similar shape formed 2 h after fusion. Scale bar 100 µm. Results observed in 17 independent experiments. **d** SCNT oocyte spindle components immunolabeled with antibodies detecting microtubules (α-tubulin-green), centromeres (kinetochore-red) and chromosomes (DAPI-blue) and visualized under fluorescence microscope. SCNT oocytes were examined 30 min, 1 h, and 2 h after cell fusion and 1 h after activation to capture critical points of spindle formation dynamics and chromosome segregation. Scale bar 2 µm. Results observed in 3 independent experiments. **e** Representative images of abnormal spindles observed in 60% of SCNT oocytes 2 h post fusion, including small, round, and multipolar configurations Scale bar 2 µm. Results observed in 3 independent experiments. **f** Failed activation after fertilization of SCNT oocytes, as indicated by reduced PB extrusion, PN formation, cleavage and high embryonic arrest compared to controls. Bar plots show the mean of 8 independent replicate experiments. *Indicates significant ($p < 0.05$) differences between groups. Two-tailed unpaired student's t test was used for comparison. Black and white dots in the graph indicate individual values. Error bars represented as SEM.

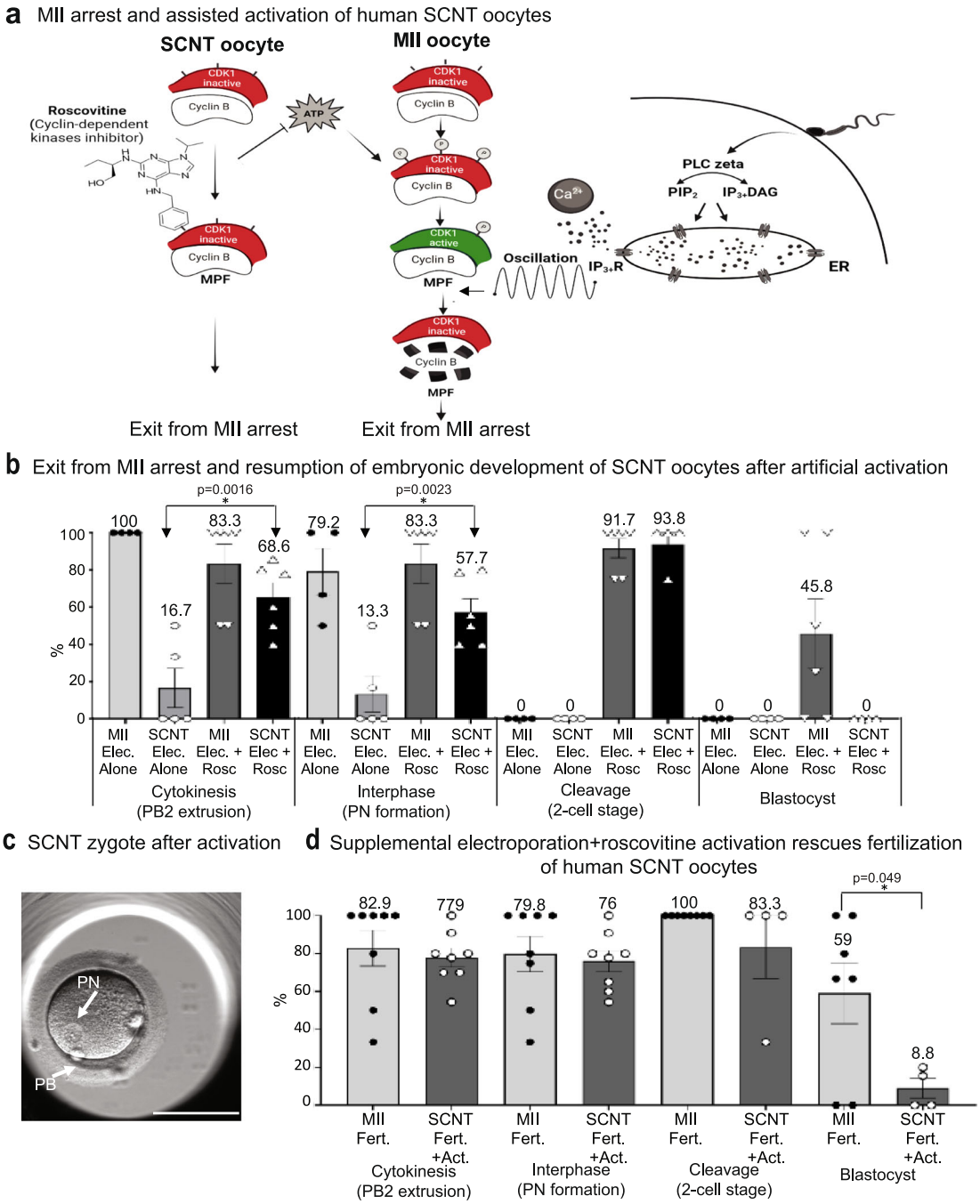

then validated the AmpliSeq on DNA samples from the study subjects confirming consistent capture between 92 and 95% of targeted genomic loci (min. 580, max. 598 of 630) necessary for determining homologous chromosome origin in SCNT oocytes and embryos (Supplementary Fig. 1a, b).

We then used daughter's skin fibroblasts arrested at the G0/G1 of the cell cycle for transfer into enucleated MII oocyte cytoplasm. Human SCNT oocytes containing visible spindles were either activated with electroporation+roscovitine or fertilized with sperm and then activated with electroporation+roscovitine and PBs and PNs or individual blastomeres of cleaving embryos were collected from each of 113 SCNT embryos. Only SCNT embryos that successfully extruded polar bodies were selected for AmpliSeq analysis. The DNA samples were processed by WGA, sequenced by AmpliSeq and the

Fig. 3 | Supplemental activation with electroporation+roscovitine can rescue the fertilization failure. a Schematic of the MII arrest mechanism and rescue of SCNT oocyte fertilization by supplemental activation with electroporation+roscovitine. Created in BioRender. Marti, N. (2025). **b** Activation and embryo development in control and SCNT oocytes after activation. Elec.- electroporation. Rosc-roscovitine treatment. Bar plots show the mean of 4 (MII with electroporation alone group), 5 (SCNT with electroporation alone group), 6 (MII with electroporation +roscovitine group) and 7 (SCNT with electroporation+roscovitine group) independent replicates. *Indicates significant ($p < 0.05$) differences between groups. Two tail unpaired student's t test was used for comparison. Black and white dots and white triangles in the graph indicate individual values. Error bars represented as SEM. **c** Bright-field (BF) image of an SCNT zygote featuring a single PN and a PB (arrows) following activation with electroporation+roscovitine. Scale bar 100 µm. Note that unfertilized but artificially activated SCNT zygotes predominantly display a single pronucleus (1 PN). In contrast, activated and sperm fertilized SCNT zygotes contain two pronuclei originating from somatic and sperm genomes. Results observed in 7 independent experiments. **d** Activation and embryo development in control and SCNT oocytes after fertilization supplemented with electroporation +roscovitine activation. Bar plots show the mean of 8 independent experiments. *Indicates significant ($p < 0.05$) differences between groups. Two tail unpaired student's *t* test was used for comparison. Black and white dots in the graph indicate individual values. Error bars represented as SEM. **e** BF image of preimplantation embryo development following SCNT oocyte fertilization supplemented with electroporation+roscovitine treatment. Left: a zygote with 2PNs and a PB. Middle: a 2-cell embryo. Right: a blastocyst. Scale bar 100 µm. Note: All SCNT zygotes that developed to blastocysts had successfully extruded polar bodies, indicating completion of mitomeiosis.

chromosomal content of 90 embryos was suitable for analysis while the remaining samples were lost during collection or sequencing. Paired analysis of both PN or blastomeres and PB revealed that in 41 (45.6%) SCNT zygotes segregation of somatic chromosomes did not occur (Fig. 4a, Supplementary data 1,2,3,4). In the majority of non-segregated embryos ($n = 39$), all 46 somatic chromosomes were retained within the PN, whereas in 2 zygotes, all chromosomes were extruded into the PB. Among the remaining 49 SCNT embryos, segregation patterns of 46 chromosomes to the daughter cells ranged from 3:43 to 23:23 (Fig. 4b, Supplementary data 1,2,3,4). We removed 8 SCNT embryos with partial segregation patterns (10 or fewer chromosomes) from the subsequent analyses to avoid artificial biases during computation of segregation patterns (Fig. 4b). Of the remaining 41 embryos, 22 provided paired, readable somatic chromosome sequences for both PN and PB compartments, while in the remaining samples clear sequencing reads were available only for PN or PB. The mean somatic chromosome count in PNs ($N = 38$) was 22.8 ± 1 while in PBs ($N = 25$) the mean count was 23.3 ± 1.3 (Fig. 4c, Supplementary data 1,2,3,4). These results suggest that partition of somatic chromosomes, consisting of single chromatids after activation of human SCNT oocytes is more or less equal. While similar to meiosis, mitomeiosis achieves numerical chromosome reduction, the random segregation pattern and absence of recombination represent fundamental differences from conventional meiotic mechanisms.

Next, we examined the segregation pattern of each 23 pairs of maternal and paternal somatic homologous chromosomes during mitomeiosis in SCNT zygotes. The mean number of properly segregated somatic homologs in PNs was 10.9 ± 2.5 and 11.1 ± 2.4 in PBs, ranging in individual SCNT zygotes from a minimum of 6 to a maximum of 16 (Fig. 4d, e, f). To evaluate the homolog segregation mechanism, we compared the distribution seen in human SCNT zygotes to a Monte Carlo simulation test calculated for random segregation of 23 pairs. The mean number of segregated homologs expected by random distribution in this simulation was 11/11.5, ranging from a minimum of 6/7 to a maximum of 16 homologous chromosomes segregated properly (Fig. 4e, f). This simulated segregation was statistically similar to that seen in SCNT zygotes, suggesting that in contrast to canonical meiosis, segregation of parental somatic homologs during mitomeiosis is random. We also analyzed segregation dynamics of individual chromosomes based on their relative length but did not observe any correlation with homolog segregation frequency (Fig. 4g). We also analyzed if chromosome morphology (metacentric vs. acrocentric) influenced segregation patterns, as recent studies have suggested differential behavior of acrocentric chromosomes in the meiotic context. However, we observed no significant correlation between chromosome morphology and segregation frequency during mitomeiosis. We next analyzed distribution of paternal vs. maternal homologs to PNs and PBs and concluded random distribution of all pairs except for chromosome 8 that showed preferential segregation of maternal homologs to PNs and paternal homologs to PBs (Fig. 4h). The bias observed for this particular chromosome segregation rates is unexpected considering that chromosome 8 is relatively moderate in size and aneuploidy rate in human IVF embryos is relatively low compared to some other chromosomes. The underlying mechanism behind this intriguing exception to the otherwise random segregation pattern for other chromosomes remains unclear and warrants further investigations.

We then analyzed all segregated somatic homologous chromosomes containing AmpliSeq reads for the entire length of chromosome for crossover recombinations. The AmpliSeq profiles of all segregated chromosomes in SCNT zygotes were identical to the original fibroblasts used for SCNT, indicating absence of recombination after mitomeiosis (Fig. 4i).

Chromosome composition in SCNT embryos produced by mitomeiosis

We next asked if SCNT zygotes produced by artificial activation can resume subsequent mitotic cell divisions and replicate somatic chromosomes. DNA isolated from individual blastomeres of nine (2–10 cell stage) cleaving SCNT embryos and DNA from pooled cells of two embryos (6–8 cell stage), were processed for sequencing. These early stage embryos were chosen to ensure accurate representation of the initial chromosome segregation patterns before additional chromosomal abnormalities potentially arising after embryonic genome activation. Single-cell chromosome analysis indicated that all 9 embryos were uniform with every sister blastomere carrying the same number and origin of somatic chromosomes (Supplementary data 3, 5). Three embryos carried the full diploid set of 46 somatic chromosomes indicating that segregation of chromosomes to the PB did not occur in these embryos (Supplementary data 3,5). The remaining 6 embryos carried a reduced number of chromosomes ranging from $N = 14$ to $N = 23$, consisting of mixture of various maternal, paternal or both parental chromosomes while some chromosome pairs were absent altogether (Fig. 5a; Supplementary data 3,5). The total number of chromosomes in two SCNT embryos from pooled cells was also reduced ($N = 34$ and $N = 41$; Supplementary data 3). These results suggest that SCNT zygotes can resume embryonic mitotic cell divisions and replicate and distribute reduced number of somatic chromosomes.

Lastly, we analyzed SCNT embryos fertilized with sperm for integration of somatic and sperm chromosomes. Analysis of pooled cell DNA from three SCNT blastocysts detected the presence of a total $N = 49$, $N = 28$, and $N = 27$ chromosomes in each embryo, respectively (Supplementary data 4 and 6). All 23 sperm homologs were present in the blastocysts, while the number and origin of somatic chromosomes varied. To determine mosaicism within sister blastomeres, we analyzed additional nine SCNT embryos at the 2–6-cell stage by single-cell sequencing of individual blastomeres.

Analysis revealed that three of these embryos were uniform while remaining six were mosaic. In uniform embryos, chromosome

https://doi.org/10.1038/s41467-025-63454-7

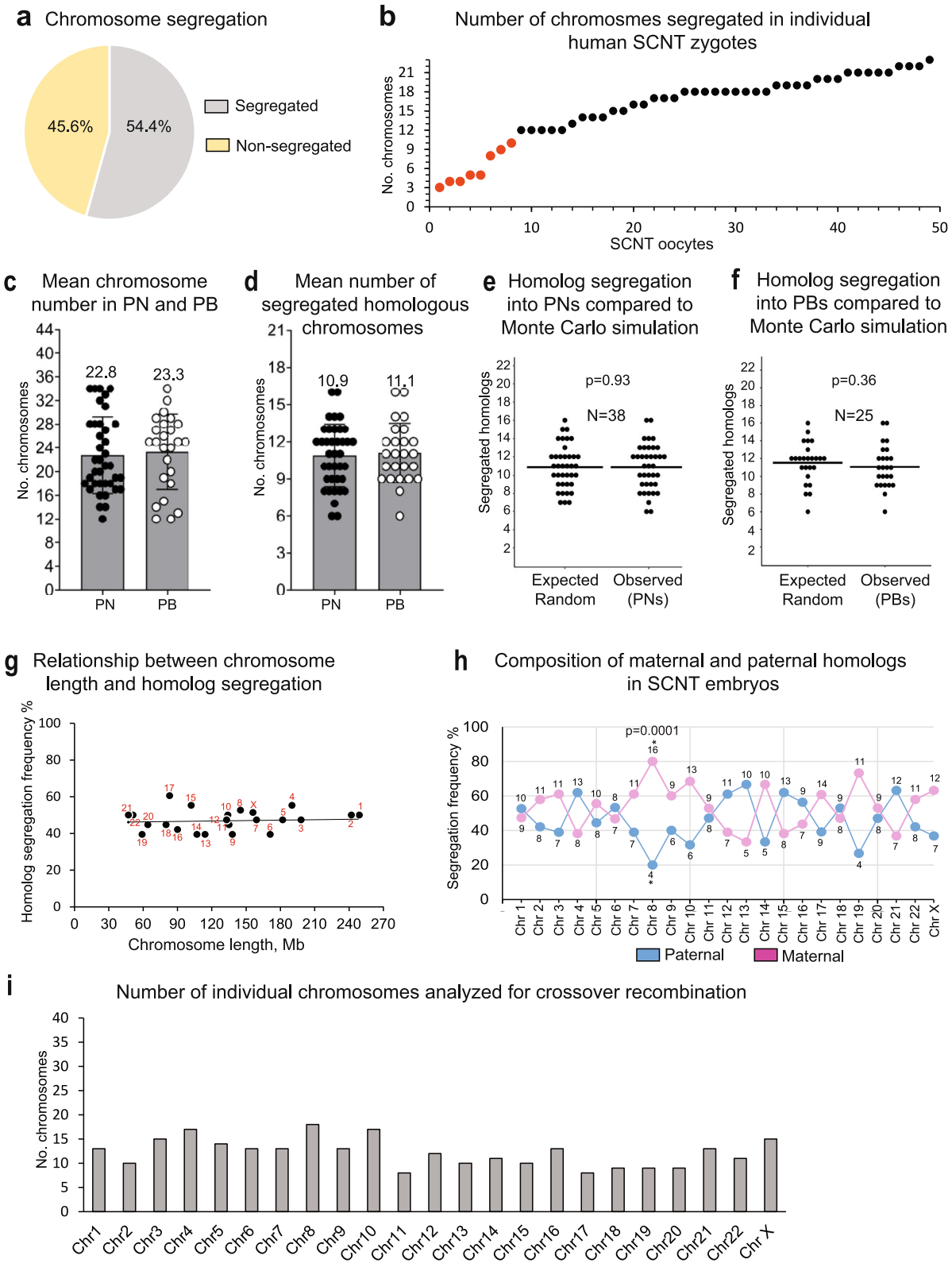

number and composition were similar among all sister blastomeres and consisted of both sperm and somatic chromosomes (Supplementary data 4 and 7). All 23 sperm homologs were present in all blastomeres of these embryos, while number and origin of somatic chromosomes varied. As expected, some somatic chromosomes were of paternal or maternal origin while for other chromosomes both homologs were present or absent (Fig. 5b, Supplementary data 4, 7). Mosaic embryos consisted of blastomeres carrying either sperm or somatic chromosomes only or mixture of somatic and sperm chromosomes (Fig. 5c, Supplementary data 4 and 8). All 23 sperm chromosomes were present in most mosaic embryos except one embryo where not all sperm chromosomes were detected. As expected, somatic cell chromosome numbers and origin varied between mosaic embryos and between sister blastomeres

Fig. 4 | Chromosome segregation and ploidy reduction of nonreplicated somatic genomes in SCNT oocytes following mitomeiosis. a Percentage of SCNT zygotes with segregated and non-segregated somatic chromosomes ($N = 90$). **b** Somatic chromosome counts in individual SCNT zygotes ($N = 49$). Each dot represents an individual SCNT zygote. Red dots indicate zygotes removed from the subsequent segregation pattern analyzes. More detailed segregation results for each zygote are presented in Supplementary data 1, 2, 3, 4. **c** Mean number of chromosomes counts in PNs and PBs of SCNT zygotes. Only somatic chromosomes derived from SCNT oocytes (without sperm chromosomes) are analyzed. Black and white dots in the graph indicate individual values. PN ($N = 38$); PB ($N = 25$) collected from 14 independent experiments. Error bars represented as SEM. **d** Mean number of segregated homologous chromosomes in PNs and PBs. Black and white dots in the graph indicate individual values. PN ($N = 38$); PB ($N = 25$) collected from 14 independent experiments. Error bars represented as SEM. **e** Comparison of homolog segregation pattern observed in PNs ($N = 38$) with random segregation pattern derived by the Monte Carlo simulation. Horizontal lines represent the mean; ($p = 0.93$, Wilcoxon rank sum test). **f** Comparation of homolog segregation pattern observed in PBs ($N = 25$) with random segregation pattern derived by the Monte Carlo simulation. Horizontal lines represent the mean; ($p = 0.76$, Wilcoxon rank sum test). **g** No linear relationship was found between chromosome length and homolog segregation frequency; $R^2 = 0.02$. **h** Random distribution of maternal and paternal homologs to PNs and PBs for all chromosomes except the chromosome 8 that showed preferential segregation of maternal homologs to PNs and paternal homologs to PBs. *Indicates significant ($p < 0.05$) differences between groups. Chi-square test was used for comparison. **i** Number of segregated homologs analyzed for each chromosome pair for detecting crossover recombinations. Note: only SCNT zygotes that extrude polar bodies were included for analyses. Note: analysis focuses on somatic-origin chromosomes only; sperm chromosomes in fertilized samples are present but excluded from this segregation analysis to enable aggregation between fertilized and non-fertilized SCNT oocytes.

ranging from $N = 46$ (diploid) to $N = 6$ and consisting of mixture of maternal, paternal and both somatic homologs.

To assess genomic stability following mitomeiosis, we performed detailed chromosome analyses of polar bodies and embryos derived from fertilized or activated SCNT oocytes (Fig. 5 and Supplementary data 3–8). Our results indicate that mitotic cycles after mitomeiosis proceed normally, with both somatic and sperm chromosomes replicating faithfully despite initial aneuploidy. In uniform embryos, chromosome numbers and composition were consistent among all sister blastomeres, suggesting stable maintenance of the initial chromosomal content throughout early embryonic divisions.

Overall, our results suggest that somatic and sperm chromosomes can integrate into a joint genome in some SCNT embryos, while in others the two genomes segregated to different sister blastomeres and formed a mosaic embryo. Despite contribution of all 23 sperm homologs, random segregation and allocation of somatic homologs to the PN of SCNT zygotes resulted in aneuploid SCNT embryos.

Discussion

The diploid genome of mammalian cells is organized as a set of chromosome pairs consisting of nearly identical parental chromosomes initially formed during fertilization of haploid oocyte with haploid sperm[20]. Reverse diploidy reduction to haploidy occurs naturally only in gamete precursors following the reductive meiosis I division. In prophase of female meiosis I, duplicated chromosomes, each consisting of two sister chromatids, undergo extraordinary rearrangements by sensing, recognizing and pairing with their homologs followed by crossover recombination[21]. These homolog alignment and crossover events collaborate with sister chromatid cohesion to create temporary physical links, called chiasmata, that connect homologs and allow them to orient and subsequently segregate one parental homolog into the MII oocyte and another into the PB1, thereby achieving haploidy. The reductional meiosis I is followed by an equational meiotic II division where, similar to mitosis, sister chromatids are segregated to opposite spindle poles eliminating one set into the PB2. Human oocyte haploidization is also an extremely long process initiating meiosis I in the first trimester of fetal development and completing the meiosis II roughly 12 or more years later, after the fertilization. Prophase I is considered the longest stage compared to other meiotic stages[22]. Mirroring these mechanistically complex and lifelong meiotic processes of natural oogenesis for human IVG remains challenging.

We have successfully utilized the residual metaphase activity and meiotic machinery in the cytoplasm of enucleated human MII oocytes to implant donor MII spindles[23] (known as spindle transfer) or PB1 genomes[24] (PB1 transfer) to induce de novo spindle formation. Moreover, such reconstructed human MII oocytes (1n2c) can readily be fertilized with sperm followed by exit from the MII arrest, segregation of sister chromatids and formation of normal diploid zygotes containing 1n1c sperm and 1n1c oocyte chromosomes[23–26]. Applications of the spindle transfer, generally known as cytoplasmic/mitochondrial replacement therapy or MRT, has been already tested in clinical IVF for treatment of female infertility and resulted in birth of healthy children[27].

Here, we explored the metaphase machinery of enucleated MII oocytes to induce reductive cell division and chromosome count reduction in the transplanted somatic genome. As indicated above, transition through different phases of the cell cycle is closely coordinated with DNA replication, chromosome duplication and distribution of chromosomes to daughter cells. This coordination is controlled by a system of cell cycle checkpoints including in G2 that prevents entry into the M-phase if DNA replication is incomplete and chromosomes are not duplicated[28]. Direct transfer of somatic cell nuclei arrested at the G0/G1 phase into the MII-arrested oocyte cytoplasm bypasses this checkpoint and induces formation of MII-like bipolar spindles in SCNT oocytes. However, human SCNT oocytes did not respond to the conventional activation stimulus induced by fertilization with sperm, failing to form zygotes. While the precise nature of this persistent metaphase arrest requires further investigation, we investigated artificial activation as supplement for fertilization with sperm.

We previously showed that fertilization of mouse SCNT oocytes provides sufficient activation signaling for release from the metaphase arrest and formation of SCNT zygotes. This suggests that interspecies differences in SCNT spindles exist between mouse and human oocytes. Therefore, we investigated supplemental activation stimuli to bypass the MII arrest in human SCNT oocytes. We demonstrate that activation by electroporation followed by incubation with cyclin-dependent kinase inhibitor roscovitine alone or in combination with sperm fertilization is required to circumvent the MII arrest and induce reductive cell division in human SCNT oocytes.

Approximately half the chromosomes from the 2n2c diploid set in human SCNT oocytes were retained within the zygote while the other half was discarded to the PB. While the average number of chromosomes after the reductive division was comparable to the haploid set, comprehensive parental chromosome sequencing indicated that the distribution of somatic homologs to the SCNT zygotes and PBs was random. Based on our recent mouse study, the sequence differences between homologs from the divergent mouse strains correlated with random segregation while proper segregation of homologs was only observed in mouse SCNT oocytes generated from inbred somatic cells[12].

Fertilized human SCNT embryos were diploid (one somatic and one sperm chromosome) for approximately half the homologs while other chromosome pairs were either triploid (two somatic and one sperm) or monosomic (sperm only). Another principal difference of mitomeiosis from the meiosis I is the lack of crossover recombinations between homologs, a source of genetic diversity in gametes.

a Uniform SCNT embryo #89 produced by activation (no sperm)

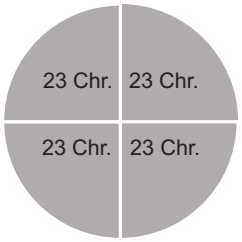

Chromosome composition
- Somatic-Paternal: 6,9,11,12,15
- Somatic-Maternal: 2,3,5,13,17,19,21,22
- Somatic-Both: 4,7,8,14,20

b Uniform SCNT embryo #10 produced by fertilization+assisted activation

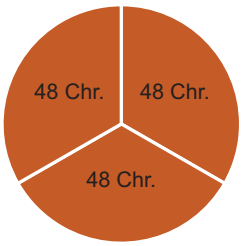

Chromosome composition
- Sperm: all 23
- Somatic-Paternal: 4,7,12,22
- Somatic-Maternal: 5,6,16
- Somatic-Both: 1,8,9,13,15,17,19,21,X

c Mosaic SCNT embryos produced by fertilization+assisted activation

Embryo #6

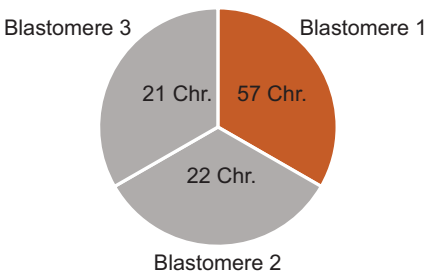

Chromosome composition in blastomere 1
- Sperm: all 23 chromosomes
- Somatic-Paternal: 5
- Somatic-Maternal: 3,12,13,14,18,20,X
- Somatic-Both: 1,2,4,6,8,10,11,15,16,17,19,21,22

Chromosome composition in blastomere 2
- Sperm: none
- Somatic-Paternal: 13,17,18,19,20,X
- Somatic-Maternal: 1,5,10,11,21,22
- Somatic-Both: 7,9,12,14,16

Chromosome composition in blastomere 3
- Sperm: none
- Somatic-Paternal: 3,5,10,11,12,18,22
- Somatic-Maternal: 7,9
- Somatic-Both: 2,6,8,13,20,X

Embryo #9

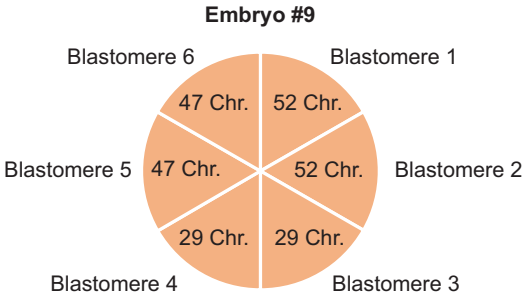

Chromosome composition in blastomeres 1 and 2
- Sperm: 1,3,4,5,6,7,8,9,10,11,13,14,15,17,18,19,20
- Somatic-Paternal: 2,5,6,11,13,15,17,18
- Somatic-Maternal: 3
- Somatic-Both: 1,4,7,8,9,12,14,16,19,20,21,22,X

Chromosome composition in blastomeres 3 and 4
- Sperm: 2,3,5,9,12,16,18,X
- Somatic-Paternal: 3,4,22,X
- Somatic-Maternal: 1,9,20
- Somatic-Both: 6,10,11,12,13,17,19

Chromosome composition in blastomeres 5 and 6
- Sperm: 1,2,4,6,7,8,10,11,12,13,14,15,16,17,19,20, 22,X
- Somatic-Paternal: 1,2,5,9,15,18,20
- Somatic-Maternal: 4,6,11,13,17,X
- Somatic-Both: 3,7,8,10,14,16,21,22

Fig. 5 | Chromosome contents in sister blastomeres of uniform and mosaic SCNT embryos. a Uniform 4-cell stage SCNT embryo #89 produced by artificial activation alone. AmpliSeq detected presence of 23 somatic chromosomes in every blastomere with random homolog segregation. **b** Uniform 3-cell stage SCNT embryo #10 produced by fertilization with sperm assisted with activation. Sequencing data show presence of all 23 sperm chromosomes and 25 somatic chromosomes in each blastomere. **c** Mosaic SCNT embryos #6 and #9 produced by fertilization with sperm assisted with activation. Individual sister blastomeres carried various number of sperm and somatic chromosomes.

Consequently, substantial further experimental modifications of the mitomeiosis will be required to achieve reductive cell division outcomes similar to the meiosis I. As mentioned above, crossover recombination and haploidization are preceded by homologous chromosomes pairing and alignment during the meiotic prophase I[21]. However, mechanisms controlling this critical and fundamental stage of meiosis are poorly understood[29]. It is believed that in most species including mammals, mechanisms responsible for crossover recombination also promote homolog pairing by delivering the machinery required for reading and detecting DNA sequence homology[29,30]. Meiotic recombination, in turn, is dependent on programmed DNA double-strand breaks (DSBs) induced across all chromosomes at multiple loci and catalyzed by the Spo11 protein[31]. The location and number of DSBs are determined by the DNA-binding specificity of the PRDM9 methyltransferase and the ATM kinase[32,33]. Meiotic DSBs recruit high-fidelity DNA repair machinery by homologous recombination including the ubiquitously expressed RAD51 DNA recombinase and the meiosis-specific DMC1 DNA recombinase which search for a homologous repair template[34]. The subsequent repair of DSBs results in either crossover or no non-crossover (gene conversion) recombination between homologous chromosomes[30]. It is likely that many of these critical components of meiosis I are absent in the MII oocyte cytoplasm thus precluding somatic homolog pairing and accurate segregation in human SCNT oocytes. Additionally, the structural complexity hypothesis suggests that the condensed, differentiated state of somatic chromatin may prevent homolog recognition mechanisms that operate during natural meiosis. As somatic genome carries complex epigenetic modifications and higher-order chromatin organization, this could impede the molecular machinery required for homolog pairing and synapsis. Moreover, meiosis naturally operates with duplicated homologs each consisting of two sister chromatids, while SCNT spindles consist of non-duplicated chromosomes. Translation of the SCNT technology for IVG applications will require addressing these and other important characteristics of gamete biology and development of novel methods for segregating somatic cell chromosomes.

Despite incomplete haploidy, somatic chromosomes retained within human SCNT zygotes enter the S-phase, duplicate and resume typical embryonic mitotic cycles. Remarkably, a semi-haploid somatic chromosome set is accurately replicated and segregated to daughter blastomeres in SCNT embryos evading further cell cycle checkpoint control mechanisms. Moreover, the somatic genome can functionally integrate with sperm chromosomes after fertilization of human SCNT oocytes and form uniform embryos consisting of somatic and sperm chromosomes.

An important limitation of our current study is the inability to distinguish between developmental arrest caused by chromosomal abnormalities versus incomplete epigenetic reprogramming of somatic chromosomes. Given that all analyzed embryos exhibited chromosomal imbalances, separating aneuploidy effects from reprogramming defects remains challenging. The modest 8.8% blastocyst development rate likely reflects contribution from both factors. Success of SCNT relies on the erasure of somatic epigenetic programs and establishment of totipotency in SCNT embryos, thus extensive future investigations are required to elucidate potential reprogramming errors before considerations of clinical applications.

Methods

Study oversight

The OHSU Institutional Review Board (IRB) reviewed, approved and provided regular oversight of this research study. In addition, a Data Safety Monitoring Committee (DSMC) was formed that provided bi-annually review of all gamete and tissue donations, use of samples, and any adverse events in study participants. During this study, 270 mature MII oocytes were utilized to generate 155 research embryos for developmental analysis and genetic characterization. No embryos were cultured beyond day 6 post-fertilization (blastocyst stage), which represents the standard timepoint for clinical embryo transfer and preimplantation genetic testing.

Ethics Statement

The study followed the guidelines regulating the use of human gametes, embryos and embryonic stem cells for research in state of Oregon set by the Oregon Stem Cell Research Oversight Committee (OSCRO) in 2008. These guidelines also regulate procurement, fertilization and genetic manipulation of human gametes, embryos and embryonic stem cells for research. The OHSU Innovative Research Advisory Panel (IRAP) and the Scientific Review Committee (SRC) reviewed and evaluated the scientific merit and ethical justification of the proposed study and recommended allowing the research with continued oversight and dialog. Members of the committees were kept confidential from the research team. The OHSU IRB supervised all committee meetings and provided documentation and formal recommendations.

Informed consent

Study subjects were provided a protocol specific consent form which included a lay language summary of the research design, approved by the OHSU IRB, prior to obtaining informed consent. The study volunteers were informed of risks associated with participation in this study, including both medical and loss of confidentiality risks. Study subjects were also provided the option to consent to be notified of any clinically relevant findings related to their genetic information, as well as whether they would allow genetic material from their donation to be shared with outside researchers.

Study participants and compensation

Healthy oocyte donors (age 21–35 years), a sperm donor and skin and blood donors were recruited locally using print flyers and online advertising. In accordance with Oregon regulations and ethical guidelines, research oocyte donors received compensation ranging from $7000 to $8000 per donation cycle, reflecting the time, effort, and potential discomfort involved in the donation process. This compensation range reflects changes over the 3–4 year study period and is consistent with amounts offered for egg donations in fertility treatments in Portland, Oregon. The study protocol, including the compensation framework, was reviewed and approved by the OHSU Institutional Review Board to ensure ethical compliance and research participant protection.

Ovarian stimulation and oocyte retrieval

Ovarian stimulation protocols and procedures were as described previously[25]. Ovarian stimulation and oocyte retrievals were managed by OHSU fertility physicians and recovered gametes were transferred to the research laboratory. All study-related procedures were conducted at the OHSU Center for Embryonic Cell and Gene Therapy. Cumulus-oocyte complexes (COCs) were treated with hyaluronidase to disaggregate and remove cumulus cells. Mature metaphase II (MII) oocytes were placed in Global Medium (Life Global) supplemented with 10% serum substitute supplement (Global 10% medium) at 37 °C in 6% CO_2 and covered with tissue culture oil (Sage IVF, Cooper Surgical).

Skin donations and fibroblast culture

Skin biopsy and blood draws were performed at OHSU fertility clinic by the study physicians. Skin punches of 1–3 mm were placed into sterile saline solution and processed to establish primary culture of fibroblasts as described earlier[35]. Fibroblasts were synchronized at the G0/G1 of the cell cycle by culturing to the full confluency and incubating in culture medium containing 0.5% FBS for 2–4 days before SCNT.

Human SCNT procedures

Oocyte enucleations and fusion with fibroblasts were performed as described previously[8]. Briefly, mature MII oocytes were place into a 30µl manipulation droplet of HTF w/HEPES (Life Global) supplemented with 10% serum substitute supplement (HTF w/HEPES 10%), containing 5 µg/ml cytochalasin B and 1.25 mM caffeine in a glass-bottom dish. Droplet was covered with tissue culture oil (Sage IVF, Cooper Surgical) and oocytes were incubated at 37 °C for 5 min before spindle removals. Dish was mounted on the stage of an inverted microscope (Olympus IX71) equipped with a stage warmer (Tokai Hit), Narishige micromanipulators, Oosight spindle imaging system and a laser objective (HamiltonThorne). An oocyte was held by a holding pipette and positioned so that the spindle was situated close to the 3 o'clock position. The zona pellucida next to the spindle was drilled with laser pulses, and an enucleation pipette was inserted through the opening. A spindle with small amount of cytoplasm surrounded by a membrane was aspirated into the pipette and discarded. A disaggregated fibroblast was aspirated into a micropipette, briefly exposed to the HVJ-E fusion extract and then placed into the perivitelline space of the cytoplast ensuring close contact with the oocyte membrane. Fused SCNT oocytes were incubated for two hours to allow spindle formation.

Fertilization by intracytoplasmic sperm injection

SCNT and MII oocytes were placed into a micromanipulation dish containing 30 µL droplet of HTF w/HEPES 10% covered with tissue culture oil and mounted on the stage of an inverted microscope (Olympus IX71) equipped with a stage warmer and Narishige micromanipulators. Fertilization was performed by intracytoplasmic sperm injection (ICSI) using frozen and thawed sperm as described previously[26].

Assisted activation of human SCNT oocytes

SCNT and MII oocytes were initially subjected to Ca^{2+} treatment by electroporation (Electro Square Porator T-820, BTX) in 0.25 M D-sorbitol buffer containing 0.1 mM calcium acetate, 0.5 mM magnesium acetate, 0.5 mM HEPES, and 1 mg/ml fatty-acid-free BSA as described before[8]. Briefly, SCNT oocytes are place between the electrodes of the BTX apparatus in D-Sorbitol buffer and subjected to two pulses (HV 3.0 kV, Pulse length 50 and 0.13 charging voltage). After electroporation, oocytes were incubated in Global 10% medium containing 50 µM roscovitine (Sigma) at 37 °C in 6% CO_2 for 4 hr. Activated SCNT oocytes were rinsed with HTF w/HEPES 10% and cultured in Global medium supplemented with 10% FBS, 12 mM b-mercaptoethanol (BME), and 10 nM Trichostatin A (TSA, Sigma) at 37 °C in 6% CO_2, 5% O_2, and 89% N_2 for 15 h in an embryoscope time-lapse incubator (Vitrolife). Time-lapse video monitoring was used to determine timing of polar body extrusions and pronuclear formations and zygotes were rinsed and cultured in Global medium supplemented with 10% FBS and 12 mM BME at 37 °C in 6% CO_2, 5% O_2, and 89% N_2.

Immunofluorescence microscopy

Zona pellucidae of SCNT and control MII oocytes was removed using a laser and oocytes were fixed in 4% paraformaldehyde for 20 min at room temperature, followed by rinsing in a blocking solution (0.3% BSA in PBS) three times for 15 min each. Fixed oocytes were permeabilized with 0.1% Triton X-100 for 20 min at room temperature and rinsed in blocking solution for 20 min at room temperature to reduce non-specific binding during subsequent antibody staining. Oocytes were incubated with antibodies for centromeres (human anti-centromere and anti-kinetochore, 1:30, Antibodies incorporated, cat#15-234) and microtubules (α-tubulin rabbit mAb AlexaFluor 488, 1:100, Cell Signaling Technology, cat#5063) washed in blocking solution and then placed on glass slides into a micro drop of mounting medium containing DAPI. A coverslip was carefully placed on top of the drop and images were analyzed with super-resolution epi-fluorescent microscope Olympus IX83 with inbuilt cellSens Dimension software. Pictures acquired with Olympus cellSens Dimension software were used to produce the rotating 3D videos using ImageJ Fiji software.

Time-lapse video

Three to four hours before filming, culture dishes were prepared with pre-equilibrated medium at 37 °C in 6% CO_2, 5% O_2, and 89% N_2 to ensure optimal medium conditions and pH. Embryos were placed individually into each well, and dishes were loaded into the EmbryoScope time-lapse incubator (Vitrolife, Sweden). The time of oocyte activation or fertilization was the start point. Embryo development was continuously monitored using integrated EmbryoViewer software v.5.4. The system captures high-resolution images of each embryo every 15-min intervals in various focal planes, allowing non-invasive, non-disturbed observation throughout the preimplantation period.

PB, PN and single blastomere collection and whole genome amplification

Zona pellucidae from zygotes and cleaved embryos were removed by brief exposure to acidic Tyrode solution (NaCl 8 mg/ml, KCl 0.2 mg/ml, $CaCl_2.2H_2O$ 2.4 mg/ml, $MgCl_2.6\ H_2O$ 0.1 mg/ml, glucose 1 mg/ml, PVP 0.04 mg/ml). Zona-free zygotes and embryos were briefly treated with trypsin (0.15% in PBS containing EDTA but Ca^{+2} and Mg^{+2} free) to loosen blastomeres and PBs. Zygotes were placed in a droplet of HTF w/HEPES 10% containing 5 µg/ml cytochalasin B and 10 µg/ml nocodazole. Pronuclei and PBs from SCNT and control zygotes were micro-surgically isolated using micromanipulators. Cleaved embryos were manually disaggregated into single blastomeres with a small-bore pipette. Individual blastomeres and isolated PNs and PBs were transferred into 0.2-ml PCR tubes containing 4 µl PBS and placed into −80 °C freezer until further use. Whole-genome amplification was performed employing multiple displacement amplification using the REPLI-g Single Cell Kit (Qiagen), following the manufacturer's manual.

Whole genome sequencing and Ampliseq design

Whole genome sequencing and AmpliSeq design were conducted to identify genomic loci capable of distinguishing between paternal and maternal homologous chromosomes of fibroblasts as nuclear donors for SCNT and from the sperm chromosomes. DNA extracted from nuclear donor fibroblasts and blood samples from both proband's parents and the sperm donor, was normalized to 500 ng in 25 µl of resuspension buffer RSB. Library preparation was carried out using the Illumina TruSeq DNA Nano kit according to the manufacturer's protocol. Paired-end sequencing was performed at 2 × 150 bp with an average autosome coverage depth of 27X using the Illumina NovaSeq 6000 platform.

Preprocessing of the raw sequencing reads was performed using the Genome Analysis Toolkit (GATK). This involved several steps: generating unaligned BAM files using FastqToSam (Picard tools v2.26.9), marking adapters with MarkIlluminaAdapters, converting unaligned BAM to fastq using SamToFastq, mapping to the GRCh38 genome assembly with BWA-MEM (v0.7.17), and merging BAM and unaligned BAM with MergeBamAlignment. The aligned reads were then coordinate-sorted using SortSamSpark (GATK v4.2.6.1), and duplicate reads were marked with MarkDuplicatesSpark (GATK v4.2.6.1). Joint variant calling was performed using FreeBayes (v1.3.5) with local left-alignment of indels, followed by normalization with bcftools (v1.14). Additional filters (QUAL > 1 & QUAL/AO > 10 & SAF > 0 & SAR > 0 & RPR > 1 & RPL > 1) were applied to remove low-confidence calls. The resulting variant sets were used for downstream analysis and identification of unique triallelic loci in R (v4.0.3).

The genomic positions of these loci were used to design a custom targeted sequencing (AmpliSeq) panel. This panel targeted 651 genomic regions across all chromosomes. Among these, 583 targeted

genomic regions contained either single nucleotide variants differentiating maternal, paternal, and sperm chromosomes, or a defined set of adjacent biallelic variants that, when phased, determined the haplotype of maternal, paternal, or sperm origin. Due to the low number of informative triallelic haplotypes, chromosomes 19, 21, and 22 were supplemented with 47 biallelic variants differentiating maternal and paternal homologs only. The average amplicon length was 260 bp, and the total length of all targeted regions was approximately 39 Kb.

AmpliSeq sequencing and chromosome segregation analysis

To analyze the chromosome content of collected PNs, PBs and blastomeres, whole genome amplified DNA concentrations were normalized to 10 ng/µl, and 50 ng input was utilized for library preparation with the AmpliSeq panel and the AmpliSeq Library PLUS kit (Illumina), following the manufacturer's protocols. Paired-end sequencing was conducted on either the Illumina MiSeq platform as 2 × 200 bp or on the Nextseq1000 as 2 × 150 bp to achieve a median coverage depth of 95X.

Preprocessing steps were applied to the raw sequencing reads using GATK to generate BAM files suitable for further analysis. These steps included generating unaligned BAM files via FastqToSam (Picard tools v2.26.9), marking adapters using MarkIlluminaAdapters, converting unaligned BAM to fastq via SamToFastq, mapping to the GRCh38 genome assembly with BWA-MEM (v0.7.17), and merging BAM and unaligned BAM with MergeBamAlignment. Duplicate reads were retained. Genomic variants were called using FreeBayes (v1.3.5), followed by normalization with bcftools (v1.14). The resulting variant calling data were then employed for downstream analysis of chromosome segregation in R (v4.3.0). Genomic loci with variant coverage depth of less than 22× were considered not amplified and were therefore excluded from the inference of chromosome origin.

Statistical analyses

Statistical analyses were performed using GraphPad Prism. Chi-square test was used for the comparison between maternal and paternal segregation. Monte Carlo Simulation was use for random segregation. Unpaired *t* test was used for comparison of mean length and width of the novo spindles, PB2 extrusion, PN formation, cleavage and blastocyst development, which were presented as mean ± SEM. Significance was set at $P < 0.05$.

Reporting summary

Further information on research design is available in the Nature Portfolio Reporting Summary linked to this article.

Data availability

All data supporting the findings of this study are included in this published article and its supplementary information files. All data used to generate summary graphs and figures are provided in Supplementary data. Due to OHSU IRB retsrictions and Oregon laws as well as terms of the consents signed by research participants, we are unable to publicly upload and share whole-genome and amplicon sequencing data outside of the OHSU network as these data sets may be used to reveal the genetic identity of the study participants. Nevertheless, we are willing to share this information on a case-by-case basis, onsite at OHSU if approval is granted by OHSU Research Integrity and the IRB (Kara Drolet, Associate VP, ORIO irb@ohsu.edu). Additionally, the approved requestor will be directed to an OHSU compliance officer to initiate a Non-Disclosure Agreement. These measures are intended to ensure the confidentiality of our research participants while also striving for research transparency and reproducibility. Upon successful approvals the requestor will be escorted by a team member at all times and granted access to an OHSU computer in a shared office where they can access and review the data sets. All requests should be initiated with OHSU Research Integrity and will move through their process, which may take upwards of 3–6 months to gain full access to all genome sequencing data that was generated in this work but not shared publicly. Source data are provided with this paper.

References

1. American College of Obstetricians and Gynecologists Committee on Gynecologic Practice and Practice Committee. Female age-related fertility decline. Committee Opinion No. 589. *Fertil Steril* **101**, 633–634 (2014).
2. Saitou, M. & Hayashi, K. Mammalian in vitro gametogenesis. *Science* **374**, eaaz6830 (2021).
3. Wilmut, I., Schnieke, A. E., McWhir, J., Kind, A. J. & Campbell, K. H. Viable offspring derived from fetal and adult mammalian cells. *Nature* **385**, 810–813 (1997).
4. Campbell, K. H., McWhir, J., Ritchie, W. A. & Wilmut, I. Sheep cloned by nuclear transfer from a cultured cell line. *Nature* **380**, 64–66 (1996).
5. Chen, M. et al. Chromatin architecture reorganization in murine somatic cell nuclear transfer embryos. *Nat. Commun.* **11**, 1813 (2020).
6. Gao, S. et al. Rapid H1 linker histone transitions following fertilization or somatic cell nuclear transfer: evidence for a uniform developmental program in mice. *Dev. Biol.* **266**, 62–75 (2004).
7. Szollosi, D., Czolowska, R., Szollosi, M. S. & Tarkowski, A. K. Remodeling of mouse thymocyte nuclei depends on the time of their transfer into activated, homologous oocytes. *J. Cell Sci.* **91**, 603–613 (1988).
8. Tachibana, M. et al. Human embryonic stem cells derived by somatic cell nuclear transfer. *Cell* **153**, 1228–1238 (2013).
9. Wolf, D. P. et al. Concise Review: Embryonic Stem Cells Derived by Somatic Cell Nuclear Transfer: A Horse in the Race?. *Stem Cells* **35**, 26–34 (2017).
10. Mitalipov, S. M., Nusser, K. D. & Wolf, D. P. Parthenogenetic activation of rhesus monkey oocytes and reconstructed embryos. *Biol. Reprod.* **65**, 253–259 (2001).
11. Lee, Y. et al. Haploidy in somatic cells is induced by mature oocytes in mice. *Commun. Biol.* **5**, 95 (2022).
12. Mikhalchenko, A. et al. Induction of somatic cell haploidy by premature cell division. *Sci. Adv.* **10**, eadk9001 (2024).
13. Ovejero, S., Bueno, A. & Sacristan, M. P. Working on genomic stability: From the S-phase to mitosis. *Genes (Basel)* **11**, https://doi.org/10.3390/genes11020225 (2020).
14. Corellou, F. et al. A S/M DNA replication checkpoint prevents nuclear and cytoplasmic events of cell division including centrosomal axis alignment and inhibits activation of cyclin-dependent kinase-like proteins in fucoid zygotes. *Development* **127**, 1651–1660 (2000).
15. Gorbsky, G. J. The spindle checkpoint and chromosome segregation in meiosis. *FEBS J.* **282**, 2471–2487 (2015).
16. Kubiak, J. Z., Weber, M., de Pennart, H., Winston, N. J. & Maro, B. The metaphase II arrest in mouse oocytes is controlled through microtubule-dependent destruction of cyclin B in the presence of CSF. *EMBO J.* **12**, 3773–3778 (1993).
17. Nurse, P. Universal control mechanism regulating onset of M-phase. *Nature* **344**, 503–508 (1990).
18. Madgwick, S. & Jones, K. T. How eggs arrest at metaphase II: MPF stabilisation plus APC/C inhibition equals Cytostatic Factor. *Cell Div.* **2**, 4 (2007).
19. Meijer, L. et al. Biochemical and cellular effects of roscovitine, a potent and selective inhibitor of the cyclin-dependent kinases cdc2, cdk2 and cdk5. *Eur. J. Biochem* **243**, 527–536 (1997).
20. Zickler, D. & Kleckner, N. Recombination, Pairing, and Synapsis of Homologs during Meiosis. *Cold Spring Harbor perspectives in biology* **7** https://doi.org/10.1101/cshperspect.a016626 (2015).

21. Schvarzstein, M., Wignall, S. M. & Villeneuve, A. M. Coordinating cohesion, co-orientation, and congression during meiosis: Lessons from holocentric chromosomes. *Genes Dev.* **24**, 219–228 (2010).
22. Bennett, M. D. The time and duration of meiosis. *Philos. Trans. R. Soc. Lond.* **277**, 201–226 (1977).
23. Tachibana, M. et al. Mitochondrial gene replacement in primate offspring and embryonic stem cells. *Nature* **461**, 367–372 (2009).
24. Ma, H. et al. Functional human oocytes generated by transfer of polar body genomes. *Cell Stem Cell* **20**, 112–119 (2017).
25. Tachibana, M. et al. Towards germline gene therapy of inherited mitochondrial diseases. *Nature* **493**, 627–631 (2013).
26. Kang, E. et al. Mitochondrial replacement in human oocytes carrying pathogenic mitochondrial DNA mutations. *Nature* **540**, 270–275 (2016).
27. Costa-Borges, N. et al. First pilot study of maternal spindle transfer for the treatment of repeated in vitro fertilization failures in couples with idiopathic infertility. *Fertil. Steril.* **119**, 964–973 (2023).
28. Sclafani, R. A. & Holzen, T. M. Cell cycle regulation of DNA replication. *Annu Rev. Genet* **41**, 237–280 (2007).
29. Bhalla, N. & Dernburg, A. F. Prelude to a division. *Annu Rev. Cell Dev. Biol.* **24**, 397–424 (2008).
30. Keeney, S., Lange, J. & Mohibullah, N. Self-organization of meiotic recombination initiation: general principles and molecular pathways. *Annu Rev. Genet* **48**, 187–214 (2014).
31. Keeney, S., Giroux, C. N. & Kleckner, N. Meiosis-specific DNA double-strand breaks are catalyzed by Spo11, a member of a widely conserved protein family. *Cell* **88**, 375–384 (1997).
32. Grey, C., Baudat, F. & de Massy, B. PRDM9, a driver of the genetic map. *PLoS Genet* **14**, e1007479 (2018).
33. Lange, J. et al. ATM controls meiotic double-strand-break formation. *Nature* **479**, 237–240 (2011).
34. Neale, M. J. & Keeney, S. Clarifying the mechanics of DNA strand exchange in meiotic recombination. *Nature* **442**, 153–158 (2006).
35. Kang, E. et al. Age-Related Accumulation of Somatic Mitochondrial DNA Mutations in Adult-Derived Human iPSCs. *Cell Stem Cell* **18**, 625–636 (2016).

Acknowledgements

We would like to thank the OHSU Institutional Review Board (IRB) and members of the Data Safety Monitoring Committee (DSMC) for oversight and guidance of this project. We are grateful to the study participants for gamete and tissue donations and staff of the Women's Health Research Unit, IVF laboratory, University Fertility Consultants, the Reproductive Endocrinology and Infertility Division in the Department of Obstetrics and Gynecology, OHSU and Spring Fertility for their assistance in procurement of human gametes. We would like to thank Evident Scientific for providing their fluorescence microscope. We are grateful to Rebecca Tippner-Hedges, former member of our laboratory, for her dedicated efforts and assistance during early stages of this research project. The studies were supported by grants from Open Philanthropy, Haploid Gamete Research Foundation, Longevity Impetus and OHSU institutional funds.

Author contributions

N.M.G., A.M., M.S., P.A. and S.M. conceived hypothesis and designed study protocols. A.K., C.V.D. and D.Y. coordinated recruitment and consenting of gamete donors. T.O.L., D.L., S. L., D.W., E.R., and P.A. conducted ovarian stimulations and oocytes retrievals. N.M.G., S.M., M.S., Z.S. and D.L. performed SCNT, fertilization, activation, embryo culture, blastomere and ESC isolations. D.F., Y.L., D.E., C.V.D., H.M. and S-G.L. performed DNA extractions, WGS and library preparation. A.M. performed Ampliseq analysis. M.S., N.M.G., Z.S., S-G.L., E.K. and Y. Lee performed immunostaining and image analyses. N.M.G., A.M., and S.M. analyzed the data and wrote the manuscript. S.M. and P.A. acquired research funding and supervised this project.

Competing interests

The authors declare no competing interests.

Additional information

Supplementary information The online version contains supplementary material available at https://doi.org/10.1038/s41467-025-63454-7.

Correspondence and requests for materials should be addressed to Paula Amato or Shoukhrat Mitalipov.

Peer review information *Nature Communications* thanks Pasqualino Loi, and the other, anonymous, reviewer(s) for their contribution to the peer review of this work. A peer review file is available.